# Effective improvement in the etching characteristics of Si{110} in low concentration TMAH solution

*Veerla Swarnalatha* ✉, *Avvaru Venkata Narasimha Rao, Prem Pal*

*MEMS and Micro/Nano Systems Laboratory, Department of Physics, Indian Institute of Technology Hyderabad, Hyderabad, India*

✉ *E-mail: ph14resch11005@iith.ac.in*

Published in Micro & Nano Letters; Received on 18th August 2017; Revised on 22nd March 2018; Accepted on 23rd April 2018

An aqueous tetramethylammonium hydroxide (TMAH) solution is widely used for silicon wet anisotropic etching to perform bulk micromachining for the fabrication of microstructures on a silicon wafer. To reduce the etching time to increase the productivity, etchant must provide high etch rate. In the present work, the etching characteristics of Si{110} in low concentration TMAH (5 wt%) with the addition of various concentrations (5–20%) of reducing agent hydroxylamine ($NH_2OH$) have been studied to increase the etch rate of Si {110} to reduce the etch time for the fabrication of microstructures. Moreover, it is aimed to enhance the undercutting at convex corner for the fast release of the structure. The etch rate of Si{110} and the undercutting at convex corners with the addition of $NH_2OH$ increases by more than three times that in pure TMAH. In addition to the etch rate and undercutting, the effect of $NH_2OH$ on etched surface morphology is investigated systematically. The present study is focused to enhance the application of wet etching in silicon micromachining for the fabrication of various kinds of microstructures for applications in microelectromechanical systems.

**1. Introduction:** Micromachining is an extensively used technique for the formation of microstructures for microelectromechanical system (MEMS) applications [1–9]. In silicon micromachining, wet anisotropic etching gained wide popularity owing to its low cost and batch production. Although many kinds of etchants are available for silicon wet chemical etching, KOH and tetramethylammonium hydroxide (TMAH) are most widely used [10–21]. In these two etchants, TMAH is very popular because of its compatibility with complementary metal oxide semiconductor process and high etch selectivity with silicon dioxide [13, 21–23]. The etching characteristics of TMAH have been studied with different concentrations ranging from 2 to 40 wt% at different temperatures. Although the etch rate in low concentrations TMAH is more than that in high concentrations, the etched surface is full of hillocks [24]. A smooth silicon surface after etching and a constant etch rate lead to precise and reproducible production. The smooth surface can be obtained by doping the etchant with surfactants such as NC-200, NCW, and Triton-X-100 [20, 21, 24]. The etch rate is an important parameter to be considered while selecting an etchant. The low etch rate directly affects the production rate. Several methods have been proposed to increase the etch rate such as ultrasonic agitation and microwave irradiation during etching [25, 26], adding some additives [27, 28], etching at the boiling point of the etchant [29, 30]. Each method has its own pros and cons such as the ultrasonic method may rupture the fragile structures, and microwave irradiation causes damage.

The wafer manufacturers mainly produce the silicon wafer with three main crystallographic orientations namely {100}, {110}, and {111}. In wet anisotropic etching, sidewalls of the stable etched profile are formed by {111} planes as they exhibit slowest etch rate in all kinds of alkaline solutions. The exposure of the number of {111} planes and their angle with wafer surface during etching depends on the orientation of wafer surface. In the case of Si{100} wafer, four {111} planes emerge during etching along ⟨110⟩ directions and make an angle of 54.7° with wafer surface, while on Si{110} wafer {111} planes expose along six directions in which two slanted (35.3°) at ⟨110⟩ directions and four perpendiculars at ⟨112⟩ directions [1–3, 31–33]. Hence, the etching of any arbitrarily shaped mask opening on Si{100} and Si{110} wafers results in rectangular and hexagon shape cavities, respectively. The presence of vertical {111} planes makes {110} wafers very useful for some specific applications such as fabrication of microstructures with vertical and smooth sidewalls (e.g. gratings, channels, electrostatic moving-fibre switch etc.) [1–3, 34–40]. In other words, Si{110} is inevitable when a structure with a vertical sidewall needs to be fabricated using wet bulk micromachining.

In the present work, we have investigated the etching characteristics of Si{110} in low concentration TMAH without and with the addition of different concentrations of $NH_2OH$. The main objective of this work is to improve the etch rate and undercutting at convex corners which are indispensable for high productivity.

**2. Experimental:** CZ grown p-type boron doped one sided polished 4-inch Si{110} wafers with a resistivity of 1–10 Ω-cm are used. Silicon dioxide layer, which is employed as masking layer in the etching process, is deposited using thermal oxidation. The oxide layer on a silicon wafer is patterned using the photolithography process followed by oxide etching in buffer hydrofluoric acid. Subsequently, the photoresist layer is removed using acetone and the wafer is thoroughly cleaned in de-ionised (DI) water. Now the wafer is diced into $2 \times 2$ $cm^2$ rhombus shape pieces. The samples are then cleaned in $H_2SO_4$:$H_2O_2$::1:1 (i.e. piranha bath) followed by a thorough rinse in the DI water. An oxide layer grown in piranha bath is removed by dipping into 1% HF for 1 min. A circular-shaped Teflon bowl is used for anisotropic etchant. To perform etching at a constant temperature, a constant temperature water bath is used. 5 wt% pure TMAH with varying concentrations of $NH_2OH$ (5, 10, 15, and 20%) is employed to study the etching characteristics (etch rate, surface morphology, and undercutting at convex corners) of Si{110}. Etching is performed at $70 \pm 1$°C. A reflex condenser made up of glass equipped with the narrow opening is used to avoid the changes in etchant concentration during the experiment. Silicon samples are dipped in 1% HF followed by a thorough rinse in DI water prior to transferring them into etchant. This step is performed to remove any native oxide layer, which may delay the etching process. Etched samples are characterised using a 3D laser scanning microscope (OLYMPUS OLS4000), an optical microscope (OLYMPU MM6C-PC), a scanning electron




© The Institution of Engineering and Technology 2018

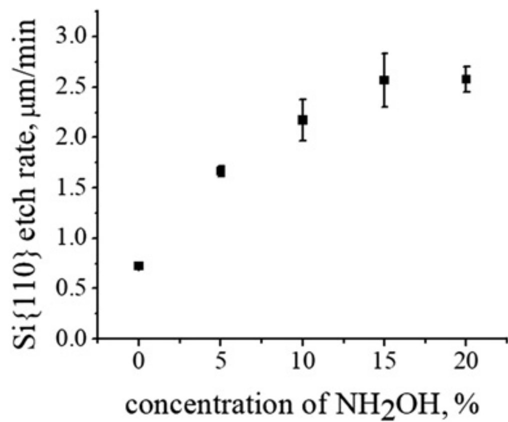


**Fig. 1** *Etch rate of Si{110} with varying concentrations of $NH_2OH$ at 70 ± 1°C*

microscope (SEM, Zeiss), and Spectroscopic Ellipsometry (J.A. Woolman Co. Inc.).

**3. Results and discussion:** The etching characteristics of Si{110} such as etch rate, etched surface morphology, and undercutting at convex corners are measured in pure and different concentrations of $NH_2OH$ added 5 wt% TMAH solution. The results are presented and discussed in the following subsections.

3.1. Etch rate: Etch rate is a very important parameter when etching is involved in the fabrication process. It is used to calculate the etching time. In this work, the etch rates of Si{110} are measured in pure and $NH_2OH$-added TMAH solution. The results are shown in Fig. 1. As the concentration of $NH_2OH$ increases, the etch rate of Si{110} increases and saturated when the concentration reaches up to 15%. The etch rate varies from 0.72 μm/min in pure TMAH to 2.58 μm/min in $NH_2OH$-added TMAH. It means the etch rate increases about 3.6 times when $NH_2OH$ is added to TMAH solution. In addition, the fluctuation in the etch rate increases with the increase of $NH_2OH$ concentration. Various parameters influence the etch rate of an etchant such as temperature, loss of reaction species ($H_2O$, $OH-$, etc.), solution stratification, diffusion transport, mask pattern spacing, and structure geometry, amount of substrate already dissolved in the etchant, etchant impurities, etching time, galvanic interaction between the etched facets [41]. When the concentration of $NH_2OH$ increases, the reactive species $H_2O$, $OH-$, and $NH_2O-$ increases. We have calculated the error bar by taking four measurements at different places on the same sample. The variation in the etch rate at different locations may be due to slight variation in one or more parameters at different places. The present research is focused to study the etching characteristics of Si{110} in pure and $NH_2OH$-added TMAH solution for applications in the fabrication of MEMS components using wet silicon bulk micromachining. The etching mechanism behind the change is the etching characteristics is not the main focus of this

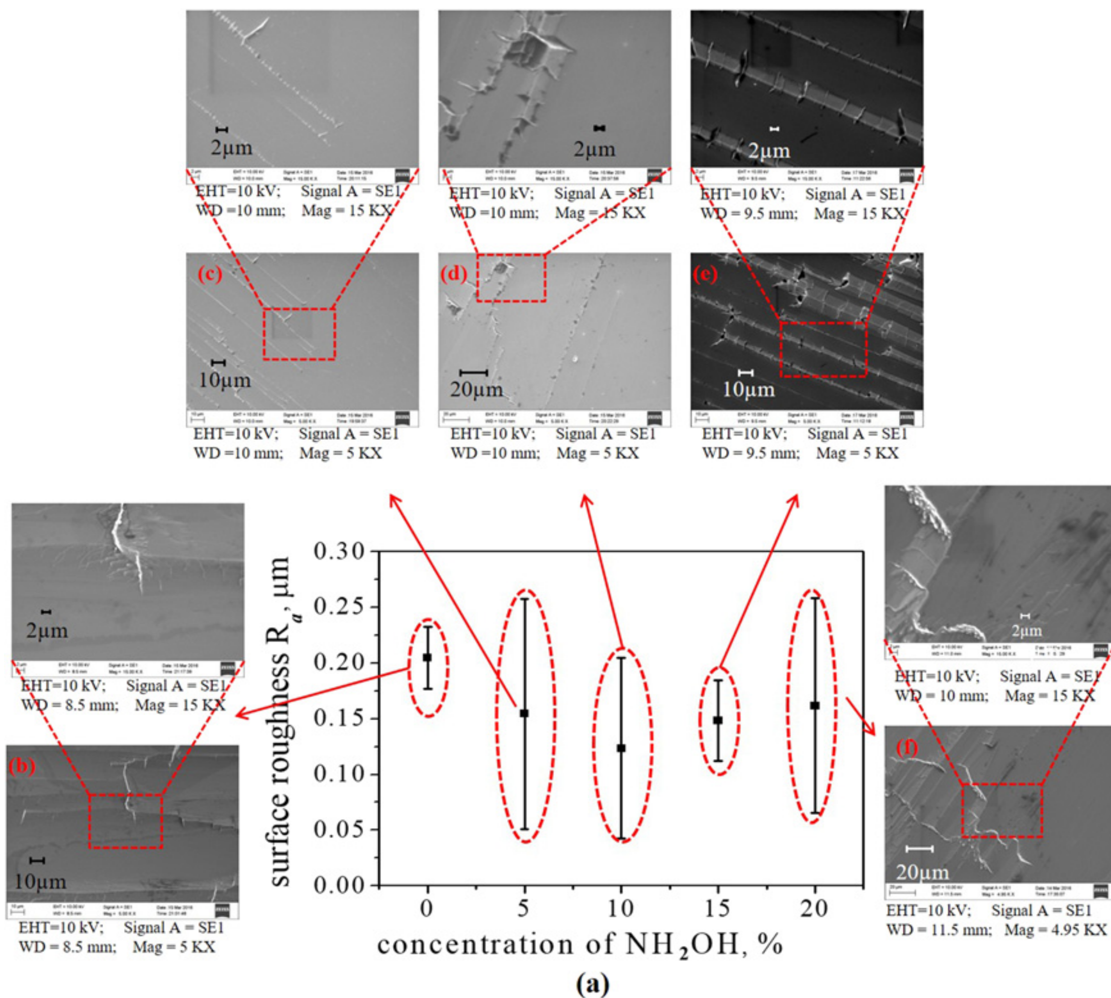


**Fig. 2** *Si{110}*
*a* Surface roughness and
*b–f* Surface morphology after etching in pure and different concentrations of $NH_2OH$-added 5% TMAH at 70±1°C. (etch time 2 h)


© The Institution of Engineering and Technology 2018

work. However, the reason for high etch rate in $NH_2OH$ added solution could be due to more accessibility of $OH^-$ ions and $H_2O$ which are available in the etching solution. This can be explained by the etching mechanism of silicon in alkaline solutions.

Etching of silicon in alkaline solutions is based on the oxidation of the silicon atoms and back-bond breaking, followed by complexation and silicate dissolution by hydronium ions. This reaction produces hydrous silica along with hydrogen gas and can be written as follows [1–3, 10, 42–44]:

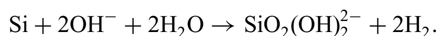

$$Si + 2OH^- + 2H_2O \rightarrow SiO_2(OH)_2^{2-} + 2H_2.$$

When $NH_2OH$ is added to TMAH (i.e. alkaline solution), it may act as an oxidising agent of silicon [45]. This can be explained by the decomposition of $NH_2OH$ in alkaline solution (e.g. TMAH) [46–48]. In the presence of alkaline solution, $NH_2OH$ reacts with $OH^-$, which gives $NH_2O^-$ ions and $H_2O$ until it reaches equilibrium condition [48–50]. Now the active species present in the etchant to remove silicon atoms are $NH_2O^-$, $OH^-$, and $H_2O$. As we know that the hydrogen-terminated silicon (Si–H) forms a bond with a hydroxyl ion (Si–OH) in pure TMAH solution, which leads to the ejection of Si atom from the surface [10]. Likewise, we speculate that the H of Si–H is replaced by $NH_2O^-$ in $NH_2OH$-added TMAH solution. Since oxygen in $NH_2O^-$ has more electronegativity than in $OH^-$, back bonds are broken at a faster rate during the etching process. Moreover, other intermediate products produced in the reaction may be participating to increase the reaction rate. This leads to the more ejection of silicon atoms that results in the enhanced etch rate.

3.2. Etched surface morphology: The etched surface morphology is the main concern for the applications related to optics and for the formation of uniform depth cavities. As discussed previously that the etched surface morphology degrades in low concentration TMAH. The surface roughness and morphologies of Si{110} samples etched in pure and $NH_2OH$-added TMAH are presented in Fig. 2. It can easily be noticed that the surface roughness is almost same in pure and $NH_2OH$-added TMAH, but the fluctuation in the surface roughness is more in $NH_2OH$-added TMAH solution. In other words, it can be stated that the addition of $NH_2OH$ does not influence surface morphology significantly. In wet chemical etching, the surface morphology of Si{110} is a result of various factors like etchant concentration and etching time [51–53], micro-masking and etchant in-homogeneities [24, 41, 54] etc. It is characterised by the formation of zigzag patterns, triangular shape hillocks on the surface. Among all the main reasons causing surface roughness in wet chemical etching, micromasking by the hydrogen bubbles and/or impurities on the surface during the etching process is a dominating factor to deteriorate the etched surface morphology [24, 41, 54–56]. Silicate particles, which are formed during etching, cling to the surface and act as a semi-permeable mask, which inhibits the

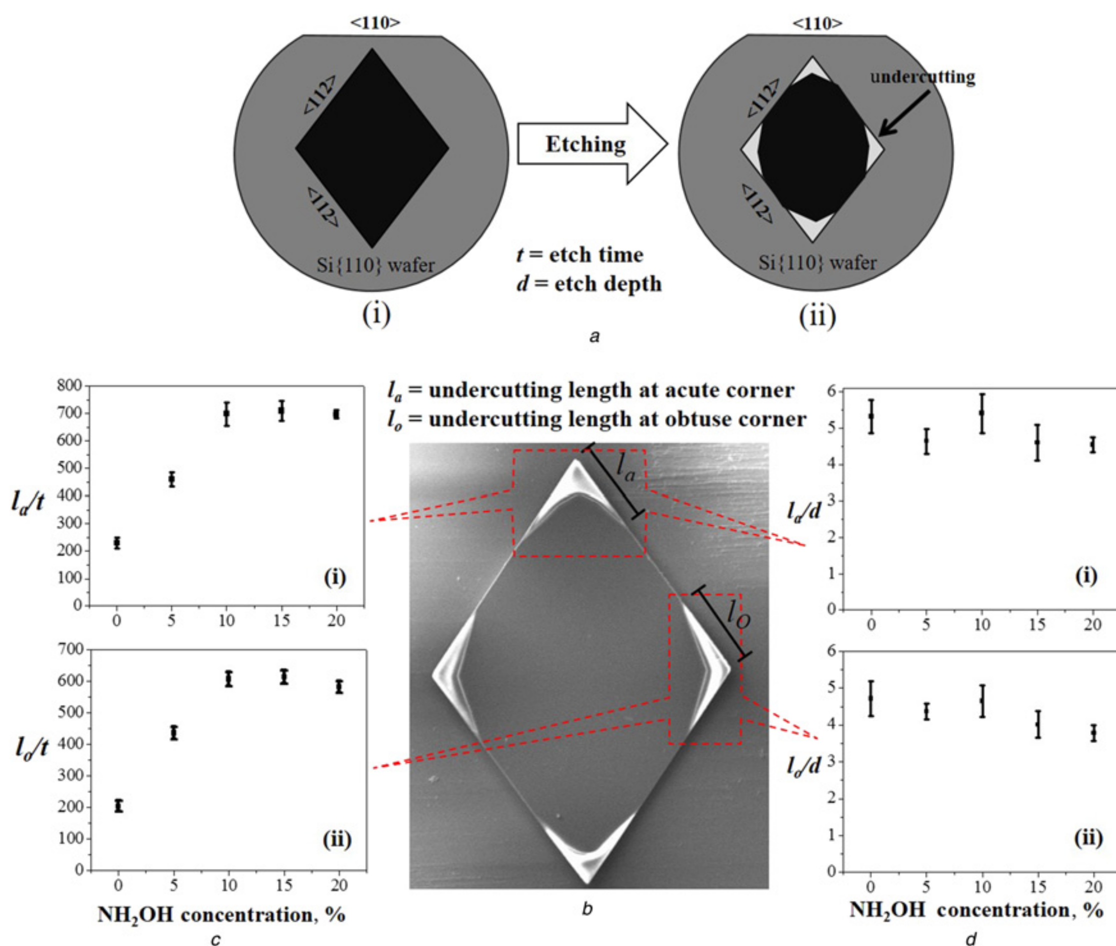


**Fig. 3** *Undercutting at convex corners*
*a* Schematic view of a mask pattern comprising convex corners (i) before etching and (ii) after etching
*b* SEM image after etching
*c* Undercutting rate (μm/h) at (i) acute ($l_a/t$) and (ii) obtuse ($l_o/t$) convex corners
*d* Undercutting ratio at (i) acute ($l_a/d$) and (ii) obtuse ($l_o/d$) convex corners etched in 5 wt% TMAH without and with varying concentrations of $NH_2OH$ at 70 ± 1°C


© The Institution of Engineering and Technology 2018

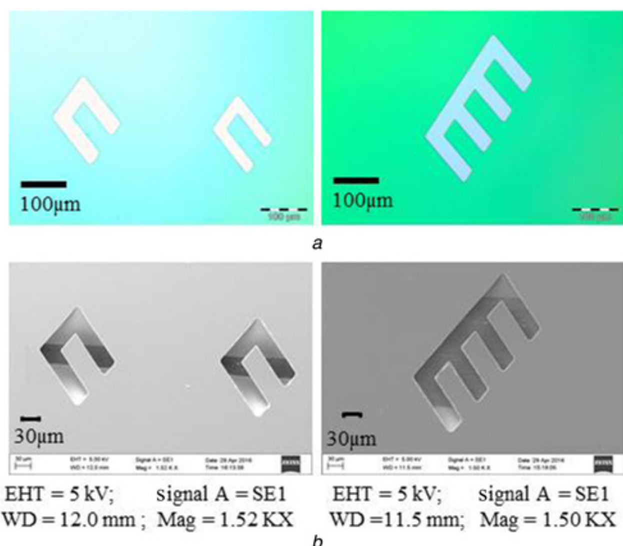


**Fig. 4** *$SiO_2$ cantilever beams released in $NH_2OH$-added TMAH*
*a* Optical image of oxide mask pattern after lithography
*b* SEM micrographs of released cantilevers

etching and initiates the zigzag pattern on the etched surface. These particles end up on the zigzag noses [55]. Figs. 2*b*–*f* show qualitative changes in the morphologies of Si{110} etched in pure 5 wt% TMAH (Fig. 2*b*) and different concentrations of $NH_2OH$-added TMAH (Figs. 2*c*–*f*). It can be seen that the etched surface comprises of broad zigzags (Figs. 2*b* and *f*), long thin zigzags (Figs. 2*c* and *d*), and patterns with crumbled noses (Fig. 2*e*).

3.3. Undercutting at convex corners: Undercutting is the lateral etching which takes place under the masking layer. It is a desirable feature at the convex corner for the fabrication of overhanging structures. For example, the realisation of suspended/freestanding microstructures made of materials such as $P^+$–Si, $SiO_2$, and $Si_3N_4$, silicon beneath a structural component needs to be removed via bulk micromachining for the application in MEMS devices. Hence, a high undercut rate is desirable for the fast release of the structure. A schematic view and the SEM image of a rhombus formed by ⟨112⟩ directions on Si{110} surface contain vertical {111} planes at the mask edges and comprises acute and obtuse corners are presented in Fig. 3. The undercutting at two different types of corners (acute and obtuse) on the Si{110} surface has been measured along the ⟨112⟩ direction using a 3D laser scanning microscope fitted with a linewidth measurement system. The undercutting rate (undercutting length ($l$)/etch time ($t$)) and the undercutting ratio (undercutting length ($l$)/etch depth ($d$)) in pure and $NH_2OH$-added 5 wt% TMAH at acute and obtuse corners are presented in Figs. 3*c* and *d*, respectively. It can easily be noticed in graphs that the undercutting rate ($l/t$) at both types of corners increases significantly when $NH_2OH$ is added to the solution. The undercutting at the convex corner is widely investigated [2, 21, 31, 33, 57–61]. All studies suggest that the undercutting at convex corner takes place due to the appearance of high etch rate planes. High etch rate planes at convex corners are usually high index planes. The increase in undercutting indicates that the etch rate of high index planes also dramatically improves when $NH_2OH$ is added into TMAH. The increment in undercutting is more than three times to that in pure TMAH. As mentioned earlier, high undercutting is advantageous for the fabrication of suspended structures. Hence, the $NH_2OH$-added TMAH is useful for the fabrication of freestanding structures. Undercutting ratio (undercutting length ($l$)/etch depth ($d$)) is an important parameter to be calculated for the design of the compensation pattern for the protection of convex corners [61]. It can easily be determined using the etch rate data and undercutting rate presented in Figs. 1 and 3, respectively.

To demonstrate the application of $NH_2OH$-added TMAH for the formation of suspended structures, $SiO_2$ cantilever beams are fabricated. Fig. 4*a* presents the optical images of cantilever beam shape structures patterned on the oxidised Si{110} wafer using photolithography and oxide etching, while Fig. 4*b* shows SEM images of suspended $SiO_2$ cantilevers on the Si{110} surface. The fabricated structures indicate that the $NH_2OH$-added TMAH, which provide high undercutting, is suitable for the fabrication of microstructures for MEMS applications.

**4. Conclusions:** Low concentration TMAH doped with varying concentration of reducing agent $NH_2OH$ has been characterised by silicon bulk micromachining to fabricate microstructures on Si{110} wafers for MEMS applications. The etchant is characterised by evaluating the etch rate, etched surface morphology, and undercutting at convex corners. 10–15% $NH_2OH$-added TMAH is an optimal choice to achieve a high etching rate and undercutting. The significant increment in the etch rate and undercutting is a very useful characteristic for the fabrication of microstructures in less time that leads to the improvement in productivity. The research presented in this study has great potential to promote the application of wet etching in MEMS.

**5. Acknowledgments:** This work was supported by research grant from the Department of Science and Technology (grant no. SR/S3/MERC/072/2011) and the Council of Scientific and Industrial Research (CSIR, grant no. 03(1320)/14/EMR-II), New Delhi, India. Sincere thanks to Prof. K. Sato, Aichi Institute of Technology Toyota, Japan for his suggestions.

## 6 References

[1] Elwenspoek M., Jansen H.V: ‘Silicon micromachining’ (Cambridge University Press, UK, 1998)
[2] Pal P., Sato K.: ‘Silicon wet bulk micromachining for MEMS’ (Pan Stanford Publishing, Singapore, 2017)
[3] Kovacs G.T., Maluf N.I., Petersen K.E.: ‘Bulk micromachining of silicon’, *IEEE Proc.*, 1998, **86**, pp. 1536–1551
[4] Ashok A., Pal P.: ‘Silicon micromachining in 25 wt% TMAH without and with surfactant concentrations ranging from ppb to ppm’, *Microsyst. Technol.*, 2017, **23**, (1), pp. 47–54
[5] Pal P., Sato K.: ‘Complex three dimensional structures in Si{100} using wet bulk micromachining’, *J. Micromech. Microeng.*, 2009, **19**, p. 105008, (9pp)
[6] Zubel I., Kramkowska M.: ‘Possibilities of extension of 3D shapes by bulk micromachining of different Si (*hkl*) substrates’, *J. Micromech. Microeng.*, 2004, **15**, (3), pp. 485–493
[7] Yang E.H., Yang S.S., Han S.W., *ET AL.*: ‘Fabrication and dynamic testing of electrostatic actuators with p+ silicon diaphragms’, *Sens. Actuators A*, 1995, **50**, pp. 151–156
[8] Lee S., Park S., Cho D.: ‘The surface/bulk micromachining (SBM) process: a new method for fabricating released microelectromechanical systems in single crystal silicon’, *J. Microelectromech. Syst.*, 1999, **8**, pp. 409–416
[9] Pal P., Sato K.: ‘Various shapes of silicon freestanding microfluidic channels and microstructures in one step lithography’, *J. Micromech. Microeng.*, 2009, **19**, (5), p. 055003, (11pp)
[10] Seidel H., Csepregi L., Heuberger A., *ET AL.*: ‘Anisotropic etching of crystalline silicon in alkaline solutions I. Orientation dependence and behavior of passivation layers’, *J. Electrochem. Soc.*, 1990, **137**, (11), pp. 3612–3626
[11] Shikida M., Sato K., Tokoro K., *ET AL.*: ‘Differences in anisotropic etching properties of KOH and TMAH solutions’, *Sens. Actuators A*, 2000, **80**, (2), pp. 179–188
[12] Zubel I., Kramkowska M.: ‘The effect of isopropyl alcohol on etching rate and roughness of (100) Si surface etched in KOH and TMAH solutions’, *Sens. Actuators A*, 2001, **93**, (2), pp. 138–147


© The Institution of Engineering and Technology 2018
doi: 10.1049/mnl.2017.0610

[13] Tabata O., Asahi R., Funabashi H., *et al.*: 'Anisotropic etching of silicon in TMAH solutions', *Sens. Actuators A*, 1992, **34**, (1), pp. 51–57
[14] Pal P., Sato K., Gosalvez M.A., *et al.*: 'Fabrication of novel microstructures based on orientation dependent adsorption of surfactant molecules in TMAH solution', *J. Micromech. Microeng.*, 2010, **21**, (1), p. 015008, (11pp)
[15] Pal P., Ashok A., Haldar S., *et al.*: 'Anisotropic etching in low concentration KOH: effects of surfactant concentration', *Micro Nano Lett.*, 2015, **10**, pp. 224–228
[16] Pal P., Sato K.: 'Fabrication methods based on wet etching process for the realization of silicon MEMS structures with new shapes', *Microsyst. Technol.*, 2010, **16**, (7), pp. 1165–1174
[17] Tang B., Yao M.Q., Tan G., *et al.*: 'Smoothness control of wet etched Si{100} surfaces in TMAH + Triton', *Key Eng. Mater.*, 2014, **609**, pp. 536–541
[18] Merlos A., Acero M., Bao M.H., *et al.*: 'TMAH/IPA anisotropic etching characteristics', *Sens. Actuators A*, 1993, **37**, pp. 737–743
[19] Resnik D., Vrtacnik D., Aljancic U., *et al.*: 'The role of Triton surfactant in anisotropic etching of {110} reflective planes on (100) silicon', *J. Micromech. Microeng.*, 2005, **15**, pp. 1174–1183
[20] Xu Y.W., Michael A., Kwok C.Y.: 'Formation of ultra-smooth 45° micromirror on (100) silicon with low concentration TMAH and surfactant: techniques for enlarging the truly 45° portion', *Sens. Actuators A*, 2011, **166**, pp. 164–171
[21] Pal P., Sato K., Gosalvez M.A., *et al.*: 'Study of rounded concave and sharp edge convex corners undercutting in CMOS compatible anisotropic etchants', *J. Micromech. Microeng.*, 2007, **17**, (11), pp. 2299–2307
[22] Zhang J., Hon W.C., Leung L.L.W., *et al.*: 'CMOS-compatible micromachining techniques for fabricating high-performance edge-suspended RF/microwave passive components on silicon substrates', *J. Micromech. Microeng.*, 2005, **15**, pp. 328–335
[23] Chen P.H., Peng H.Y., Hsieh C.M., *et al.*: 'The characteristic behavior of TMAH water solution for anisotropic etching on both silicon substrate and $SiO_2$ layer', *Sens. Actuators A*, 2001, **93**, (2), pp. 132–137
[24] Cheng D., Gosalvez M.A., Hori T., *et al.*: 'Improvement in smoothness of anisotropically etched silicon surfaces: effects of surfactant and TMAH concentrations', *Sens. Actuators A*, 2006, **125**, pp. 415–421
[25] Chen J., Liu L., Li Z., *et al.*: 'Study of anisotropic etching of (100) Si with ultrasonic agitation', *Sens. Actuators A*, 2002, **96**, (2), pp. 152–156
[26] Dziuban J.A.: 'Microwave enhanced fast anisotropic etching of monocrystalline silicon', *Sens. Actuators A*, 2000, **85**, (1), pp. 133–138
[27] Sotoaka R.: 'New etchants for high speed anisotropic etching of silicon', *J. Surf. Finish. Soc. Jpn.*, 2008, **59**, (2), pp. 104–106
[28] Yang C.R., Chen P.Y., Yang C.H., *et al.*: 'Effects of various ion-typed surfactants on silicon anisotropic etching properties in KOH and TMAH solutions', *Sens. Actuators A*, 2005, **119**, pp. 271–281
[29] Tanaka H., Yamashita S., Abe Y., *et al.*: 'Fast etching of silicon with a smooth surface in high temperature ranges near the boiling point of KOH solution', *Sens. Actuators A*, 2004, **114**, (2–3), pp. 516–520
[30] Tang B., Sato K., Zhang D., *et al.*: 'Fast Si (100) etching with a smooth surface near the boiling temperature in surfactant modified tetramethylammonium hydroxide solutions', *Micro Nano Lett.*, 2014, **9**, (9), pp. 582–584
[31] Pal P., Gosalvez M.A., Sato K., *et al.*: 'Anisotropic etching on Si {110}: experiment and simulation for the formation of microstructures with convex corners', *J. Micromech. Microeng.*, 2014, **24**, (12), p. 125001 (12pp)
[32] Singh S.S., Avvaru V.N., Veerla S., *et al.*: 'A measurement free pre-etched pattern to identify the ⟨110⟩ directions on Si{110} wafer', *Microsyst. Technol.*, 2017, **23**, (6), pp. 2131–2137
[33] Pal P., Singh S.S.: 'A new model for the etching characteristics of corners formed by Si{111} planes on Si{110} wafer surface', *Engineering*, 2013, **5**, (11), pp. 1–8
[34] Holke A., Henderson H.T.: 'Ultra-deep anisotropic etching of (110) silicon', *J. Micromech. Microeng.*, 1999, **9**, pp. 51–57
[35] Tolmachev V.A., Granitsyna L.S., Vlasova E.N., *et al.*: 'One-dimensional photonic crystal obtained using vertical anisotropic etching of silicon', *Semiconductors*, 2002, **36**, pp. 932–935
[36] Zubel I., Kramkowska M.: 'Possibilities of extension of 3D shapes by bulk micromachining of different Si (*hkl*) substrates', *J. Micromech. Microeng.*, 2009, **15**, pp. 485–493
[37] Lee D., Yu K., Krishnamoorthy U., *et al.*: 'Vertical mirror fabrication combining KOH etch and DRIE of (110) silicon', *J. Microelectromech. Syst.*, 2009, **18**, pp. 217–227
[38] Ahn M., Heilmann R.K., Schattenburg M.L.: 'Fabrication of ultra-high aspect ratio freestanding gratings on silicon-on-insulator wafers', *J. Vac. Sci. Technol. B.*, 2007, **25**, (6), pp. 2593–2597
[39] Kendall D.L.: 'Vertical etching of silicon at very high aspect ratios', *Annu. Rev. Mater. Sci.*, 1979, **9**, (1), pp. 373–403
[40] Kim S.H., Lee S.H., Lim H.T., *et al.*: 'Anisotropic bulk etching of (110) Silicon with high aspect ratio', *IEEJ Trans. Sens. Micromach.*, 1997, **118**, pp. 32–36
[41] Gosálvez M.A., Zubel I., Viinikka E.: 'Wet etching of silicon', in Markku T., Motooka T., Airaksinen V.M., *et al.* (Eds.): 'Handbook of silicon based MEMS materials and technologies' (William Andrew, Norwich, NY, USA, 2015), ch. 22, pp. 477–502
[42] Narasimha Rao A.V., Swarnalatha V., Pal P.: 'Etching characteristics of Si {110} in 20 wt% KOH with addition of hydroxylamine for the fabrication of bulk micromachined MEMS', *Micro Nano Syst. Lett.*, 2017, **5**, (1), p. 23
[43] Van Den Meerakker J.E.A.M.: 'The reduction of hydrogen peroxide at silicon in weak alkaline solutions', *Electrochim. Acta*, 1990, **35**, (8), pp. 1267–1272
[44] Schnakenberg U., Benecke W., Löchel B., *et al.*: '$NH_4OH$-based etchants for silicon micromachining: influence of additives and stability of passivation layers', *Sens. Actuators A*, 1990, **25**, (1–3), pp. 1–7
[45] Michael A.: 'The structures and reactions of hydroxylamine and its derivatives', *J. Am. Chem. Soc.*, 1921, **43**, (2), pp. 315–332
[46] Cisneros L.O., Rogers W.J., Mannan M.S.: 'Comparison of the thermal decomposition behaviour for members of the hydroxylamine family', *Thermochim. Acta*, 2004, **414**, (2), pp. 177–183
[47] Hughes M.N., Nicklin H.G.: 'Autoxidation of hydroxylamine in alkaline solutions', *J. Chem. Soc. A, Inorg. Phys. Theor.*, 1971, pp. 164–168
[48] Wei C., Saraf S.R., Rogers W.J., *et al.*: 'Thermal runaway reaction hazards and mechanisms of hydroxylamine with acid/base contaminants', *Thermochim. Acta*, 2004, **421**, (1), pp. 1–9
[49] Cisneros L.O., Wu X., Rogers W.J., *et al.*: 'Decomposition products of 50 mass% hydroxylamine/water under runaway reaction conditions', *Process Saf. Environ. Prot.*, 2003, **81**, (2), pp. 121–124
[50] Chunyang W.: 'Thermal runaway reaction hazard and decomposition mechanism of the hydroxylamine system'. PhD dissertation, Texas A&M University, 2005
[51] Lunak S., Veprek Siska J.: 'The catalytic effect of cations on the decomposition of alkaline solutions of hydroxylamine', *Collect. Czech. Chem. Commun.*, 1974, **39**, pp. 391–395
[52] Nguyen Q.D.: 'Electrochemistry in anisotropic etching of silicon in alkaline solutions'. PhD dissertation, University of Twente, 2007
[53] Shikida M., Masuda T., Uchikawa D., *et al.*: 'Surface roughness of single-crystal silicon etched by TMAH solution', *Sens. Actuators A*, 2001, **90**, (3), pp. 223–231
[54] Gosálvez M.A., Xing Y., Hynninen T., *et al.*: 'Faster simulations of step bunching during anisotropic etching: formation of zigzag structures on Si (1 1 0)', *J. Micromech. Microeng.*, 2007, **17**, (4), pp. S27–S37
[55] Van Veenendaal E., Sato K., Shikida M., *et al.*: 'Micromorphology of single crystalline silicon surfaces during anisotropic wet chemical etching in KOH and TMAH', *Sens. Actuators A*, 2001, **93**, (3), pp. 219–231
[56] Palik E.D., Glembocki O.J., Heard I.Jr., *et al.*: 'Etching roughness for (100) silicon surfaces in aqueous KOH', *J. Appl. Phys.*, 1991, **70**, (6), pp. 3291–3300
[57] Dong W., Zhang X., Liu C., *et al.*: 'Mechanism for convex corner undercutting of (110) silicon in KOH', *Microelectron. J.*, 2004, **35**, (5), pp. 417–419
[58] Pal P., Singh S.S.: 'A simple and robust model to explain convex corner undercutting in wet bulk micromachining', *Micro Nano Syst. Lett.*, 2013, **1**, (1), pp. 1–6
[59] Kim B., Cho D.D.: 'Aqueous KOH etching of silicon (110) etch characteristics and compensation methods for convex corners', *J. Electrochem. Soc.*, 1998, **145**, pp. 2499–2508
[60] Pal P., Sato K., Chandra S.: 'Fabrication techniques of convex corners in (100)-silicon wafer using bulk micromachining: a review', *J. Micromech. Microeng.*, 2007, **17**, (10), pp. R111–R133
[61] Pal P., Sato K.: 'A comprehensive review on convex and concave corners in silicon bulk micromachining based on anisotropic wet chemical etching', *Micro Nano Syst. Lett.*, 2015, **3**, (1), pp. 1–42


© The Institution of Engineering and Technology 2018